Macromolecular Rapid Communications
www.mrc-journal.de

Evaluation of Charge-Regulated Supramolecular Copolymerization to Tune the Time Scale for Oxidative Disassembly of β-Sheet Comonomers

*Christian M. Berac, Lydia Zengerling, David Straßburger, Ronja Otter, Moritz Urschbach, and Pol Besenius**

A multistimuli-responsive supramolecular copolymerization is reported. The copolymerization is driven by hydrogen bond encoded β-sheet-based charge co-assembly into 1D nanorods in water, using glutamic acid or lysine residues in either of the peptide comonomers. The incorporation of methionine as hydrophobic amino acid supports β-sheet formation, but oxidation of the thioether side-chain to a sulfoxide functional group destabilizes the β-sheet ordered domains and induces disassembly of the supramolecular polymers. Using H_2O_2 as reactive oxygen species, the time scale and kinetics of the oxidative disassembly are probed. Compared to the charge neutral homopolymers, it is found that the oxidative disassembly of the charged ampholytic copolymers is up to two times faster and is operative at neutral pH. The strategy is therefore an important addition to the growing field of amphiphilic polythioether containing (macro)molecular building blocks, particularly in view of tuning their oxidation induced disassembly which tends to be notoriously slow and requires high concentrations of reactive oxygen species or acidic reaction media.

Great progress has recently been achieved in transitioning from molecular and supramolecular materials with functional properties derived from their equilibrium structures to adaptive design features that emerge from non-equilibrium and dissipative states.[1–9] In both approaches the creativity of the chemistry community enabled the design and synthesis of a variety of artificial molecular subunits that reversibly change their properties by external stimuli and can be addressed through changes in the pH, ionic strength, redox environment, irradiation with light or enzyme catalyzed transformations.[10–16] This allows the manipulation of thermodynamic or kinetic constraints under which these molecular subunits operate. Our group has recently reported a transiently stable supramolecular polymer and hydrogelator, by coupling a charge-regulated assembly with a redox-regulated trigger.[17] Given that both operate on largely different time scales we were able to install transiently stable assembled states. Their life time is tuneable and is dictated by the concentration of the glucose oxidase (GOx) catalyst and glucose as fuel that produces protons for the fast assembly on-trigger, as well as H_2O_2 as reactive oxygen species (ROS) for the slow off-trigger. The molecular design was based on dendritic peptide amphiphiles with a β-sheet encoding oligopeptide,[18–21] using pH responsive glutamic acids and the oxidation responsive thioether side-chains of methionine. More recently, we have also extended the concept from low molecular weight supramolecular peptide monomers to ABA triblock peptide–polymer conjugates which assemble via an intramolecular folding induced intermolecular self-assembly into core–shell nanorods in water.[22] At solid weight contents above 1 wt%, hydrogels with tuneable life times between 1 h to 12 h were obtained. A number of groups have previously reported the incorporation of thioether functional groups as a strategy to prepare ROS-responsive supramolecular materials, making use of the oxidation to much more hydrophilic sulfoxide species.[23–30] Tirelli and Hubbell have reported poly(ethylene glycol)-*bl*-(propylene sulfide) di- and triblock copolymers, which assemble into micelles, rod-like micelles or polymersomes, their oxidative destabilization and disassembly.[31–35] Deming has embedded methionine amino acids in amphiphilic block copolymers that assemble into different morphologies depending on the oxidation state of the side chains.[36–38] More recently, the Frey group also extended the concept to 2-methylthioethyl substituted poly(glycidyl ether) block copolymer micelles which disassemble upon oxidation using H_2O_2.[39]

In living organisms, the pH values as well as the concentrations of ROS are stringently regulated. Oxidative stress is known to cause oxidative damage and changes in activity for

C. M. Berac, L. Zengerling, D. Straßburger, R. Otter, M. Urschbach, Prof. P. Besenius
Institute of Organic Chemistry
Johannes Gutenberg-University Mainz
Duesbergweg 10–14, 55128 Mainz, Germany
E-mail: besenius@uni-mainz.de
C. M. Berac, Prof. P. Besenius
Graduate School of Materials Science in Mainz
Staudingerweg 9, 55128 Mainz, Germany
The ORCID identification number(s) for the author(s) of this article can be found under https://doi.org/10.1002/marc.201900476.

DOI: 10.1002/marc.201900476

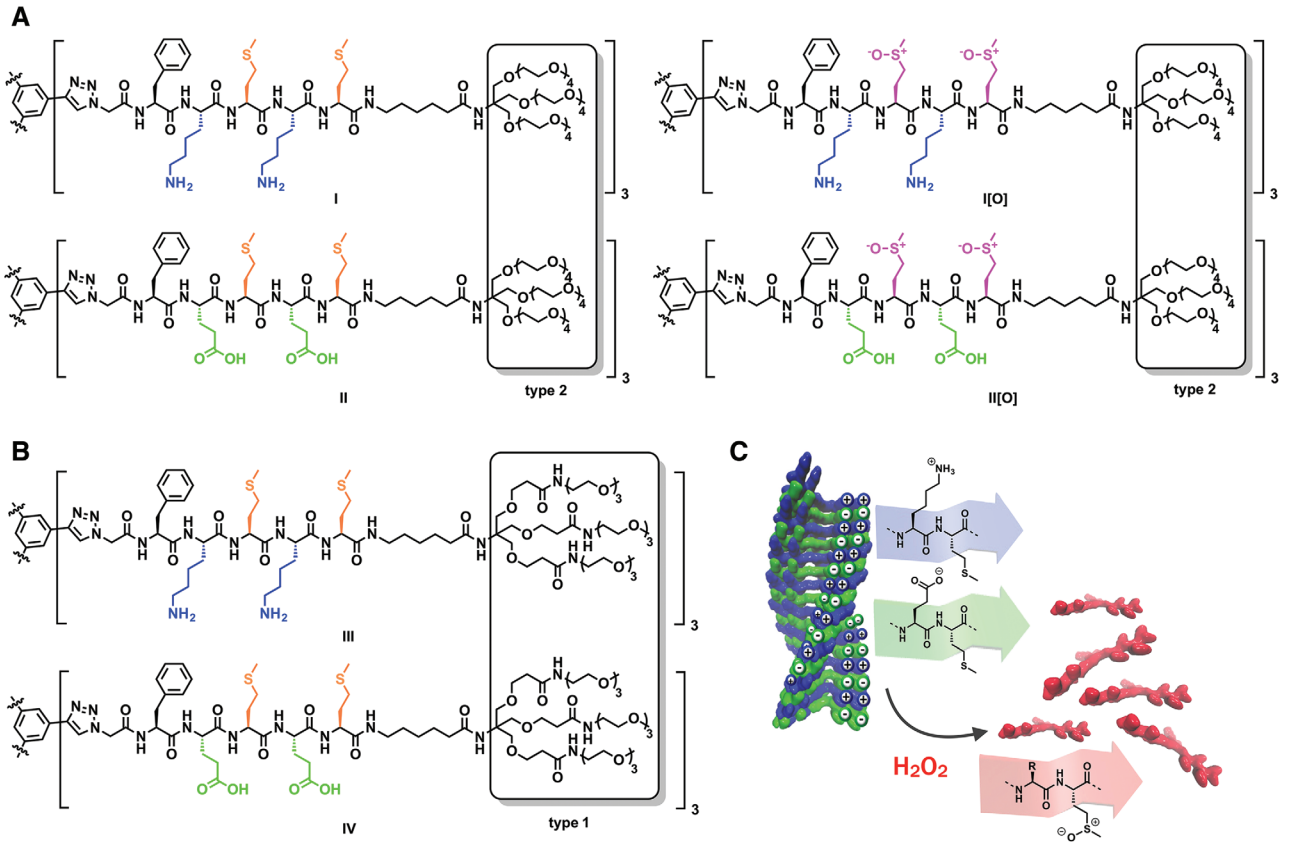

Figure 1. Schematic representation of FKMKM containing monomers I and III, of the FEMEM containing monomers II and IV, and the oxidized monomers I[O] and II[O] with the dendron type 2 A) and type 1 B), as well as a schematic representation for the oxidative disassembly of supramolecular copolymers C).

proteins.[40–42] Some enzymes are therefore able to shield and protect their environment from ROS by partial self-oxidation. Hereby, methionine (M) residues in the solvated outer protein shell are oxidized to methionine sulfoxides. In contrast, functional thioethers in synthetic supramolecular assemblies are typically embedded in desolvated hydrophobic domains and thus provide limited accessibility for oxidation reagents like H_2O_2. Inspired by the capacity of biological systems to scavenge ROS, we hereby report supramolecular copolymers that are driven by hydrogen bond encoded β-sheets, as well as attractive Coulomb interactions of glutamic acid (E) and lysine (K) residues in either of co-assembled peptide comonomers. The charged character increases the hydrophilicity of the β-sheet units, yet does not compromise their stability in neutral pH and physiological ionic strength.[19–21] Using H_2O_2 as ROS, we aim to probe the kinetics for the oxidation of the methionine units and concomitant disassembly of the supramolecular copolymers. Manipulating and tuning the oxidative disassembly and response-time of ampholytic supramolecular copolymers is an attractive strategy in the growing field of amphiphilic polythioether containing (macro)molecular building blocks,[30,43–45] particularly in view of their ROS-responsive properties which tend to be notoriously slow and require high concentrations of oxidizing reagent or acidic reaction media.

We previously reported the transient supramolecular polymerization of dendritic peptide amphiphiles using a coupled pH- and redox-regulated process.[17] The C_3-symmetric peptides contained a GFEMEM sequence connected via triazole linkages to a rigid benzene core. Note, that the additional phenylalanine (F) moiety stabilizes the supramolecular assemblies via hydrophobic shielding effects. The outer shell was solvated using a known Newkome dendron[46] and oligoethylene glycols as solubilizing chains.[17,47] Here, we aim to prepare supramolecular copolymers and use complementary comonomers incorporating anionic GFEMEM or cationic GFKMKM oligopeptide sequences. In addition to the reported Newkome dendrons where the oligo ethylene glycol chains are connected via amide groups (type 1), we further introduce a new Tris-ether linkage, referred to as dendron type 2 (**Figure 1**), in order to further decrease the steric demand[48] in the solubilizing dendritic shell.

First, we synthesized the new Newkome dendron type 2 in five steps starting with a nucleophilic substitution of 6-bromohexanoic acid (**9**) with sodium azide to 6-azido-hexanoic acid (**10**) (Figure S25, Supporting Information). After an EEDQ-mediated coupling of 6-azido-hexanoic acid (**10**) with Tris, an additional nucleophilic substitution using triethylene glycol monomethyl ether tosylate (**8**) yielded the azide functional Newkome dendron type 2 (**12**). The amine **13** was finally obtained after reduction with hydrogen over Pd/C. **13** was coupled with the side chain protected oligopeptide sequences N_3-GFE(^{t}Bu)ME(^{t}Bu)M-OH (**15**) and N_3-GFK(Boc)MK(Boc)M-OH

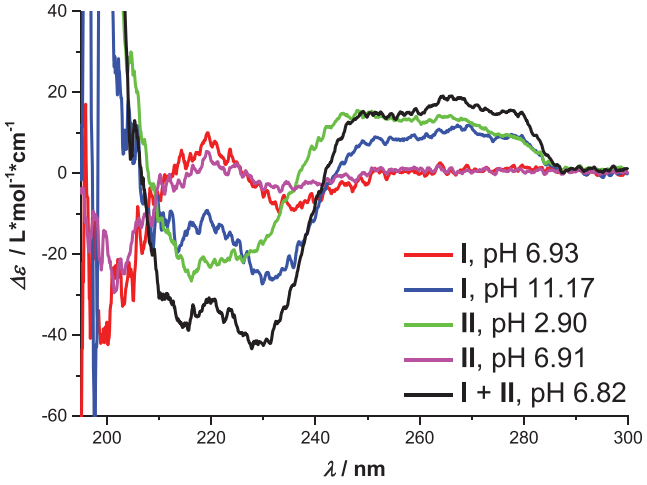

Figure 2. pH-dependent CD spectra of I, II and copolymer I + II. All CD measurements were performed with 60 μM solutions in 10 mM phosphate buffer.

(**14**) using PyBOP as coupling reagent. The dendritic scaffold was established by coupling the azide functional amphiphilic peptides (**16** or **17**) with 1,3,5-triethynylbenzene or with trimethylsilane (TMS)-protected 1,3,5-triethynylbenzene **20** using Cu^{I}-catalyzed azide-alkyne cycloaddition (CuAAC) chemistry.[49,50] Standard acid mediated deprotection of the ^{t}butyl ester and Boc protecting groups finally yielded the two dendritic peptide amphiphiles **I** and **II** (Figure 1). The synthesis of **III** and **IV** was previously reported (Figure 1).[17] The detailed synthetic procedures, full analysis, and characterization are reported in the Supporting Information.

We have previously reported the supramolecular polymerization of monomer **III** in basic, monomer **IV** in acidic media, and the formation of copolymers of **III** and **IV** at neutral pH.[19,21,51] In all cases, the polymers were shown to have anisotropic shapes, with 1D arrangement of the monomers to structures that appear as nanorods in transmission electron microscopy (TEM). In order to investigate the pH-dependent self-assembly of the monomers **I** and **II** with the new tetraethylene glycol-based dendron, we performed circular dichroism (CD) spectroscopy at different pH values (**Figure 2**). All samples were measured in 10 mM phosphate buffer at a concentration of 60 μM. At neutral pH, the CD spectra of isolated solutions of monomer **I** (red) and monomer **II** (pink) both display a strong negative band at λ = 200 nm, a weak positive band at λ = 218 nm and a weak negative band at λ = 233 nm, which is characteristic for a random-coil peptide secondary structure. We previously assigned these bands to the molecular dissolved state of the monomeric building block.[17] This result indicates that due to the Coulomb repulsion of the protonated lysine **I** and deprotonated glutamic acid **II** side chains the monomers do not form homopolymers at neutral pH. As expected, the lysine containing monomer **I** (blue) self-assembles in basic buffer (pH 11.17), as indicated by a β-sheet characteristic CD spectrum with positive bands at λ = 200, 250, 265, 277 nm, and a strong negative band at λ = 230 nm. Note, that the additional bands λ > 240 nm are most likely due to the aromatic benzene tris(triazole) core of the dendritic peptide. The β-sheet induced self-assembly is also present in the case of glutamic acid containing monomer **II** (green) in acidic medium (pH 2.90). Hereby, positive β-sheet characteristic bands at λ = 200, 250, and 265 nm as well as a negative band at λ = 215 nm were obtained. In contrast to the isolated solutions of both monomers, the CD spectrum for the mixed solution of **I** and **II** (black), gives rise to β-sheet bands in neutral phosphate buffer (pH 6.82). Strong CD signals are apparent with positive bands at λ = 200, 250, 265, and 277 nm, as well as negative bands at λ = 215 and 226 nm.

We further compared the results obtained for the pH-regulated homo- and copolymerizations of **I** and **II**, to the monomers **III** and **IV**. Both set of comonomers only differ by the type of dendron and the characteristic CD bands observed for all homopolymers and copolymers do not change significantly (Figures 2; Figure S1, Supporting Information). In order to characterize the morphology of the β-sheet directed peptidic supramolecular (co)polymers, we performed transmission electron microscopy experiments at various pH values. First, we dissolved the monomers **I** and **II** (50 μM) in 20 mM Tris buffer at neutral pH and adjusted the pH of the solution of monomer **I** with 1 M NaOH to pH 10.75 and the solution of monomer **II** with 1 M HCl to pH 1.64. In addition, the mixed comonomer solution of equimolar ratios of **I** + **II** (50 μM) was adjusted to pH 7.00. **Figure 3** shows representative TEM micrographs of **I**, **II**, and **I** + **II** (50 μM) after negative staining using uranyl acetate. In all cases charge screening either by adjusting pH for the homopolymer formation, or by co-polymerization of oppositely charged comonomers, leads to rigid nanorods of similar thickness that were observed in basic pH for **I** (Figure 3A; Figure S16, Supporting Information), acidic pH for **II** (Figure 3B; Figure S18, Supporting Information), as well as neutral pH for the copolymer **I** + **II** (Figure 3C; Figure S20, Supporting Information). Furthermore, the average contour length of the homopolymers of **I** (L_n = 65, L_w = 101, L_w/L_n = 1.6, n = 104) and homopolymers of **II** (L_n = 61, L_w = 84, L_w/L_n = 1.4, n = 112) are nearly identical. The ampholytic supramolecular copolymer **I** + **II** was noticeably longer (L_n = 101, L_w = 137, L_w/L_n = 1.4, n = 120) than the homopolymers of **I** and **II** (Figure S24, Supporting Information).

Finally, we investigated the most important aspect of the supramolecular assemblies and focused further experiments on structural as well as kinetic evaluation of the oxidation of the methionine containing peptide sequences using all monomer combinations, as well as different pH values. First, we decided to oxidize both monomers **I** and **II** to the methionine sulfoxide from a molecular dissolved state in concentrated H_2O_2, glacial acetic acid at 0 °C and standard experimental procedures from the literature, to obtain reference compounds for further detailed investigations.[17] Both monomers **I[O]** and **II[O]** with the corresponding oligopeptide sequences GFKM[O]KM[O] and GFEM[O]EM[O] were investigated for their potential to form supramolecular homo- and copolymers. In Figure S2, Supporting Information, the CD spectroscopic analysis shows that monomer **I[O]** at basic (red) or neutral pH (black), **II[O]** at acidic (blue) or neutral (pink) pH, and the mixed comonomers **I[O]** + **II[O]** at neutral (green) conditions do not give rise to CD bands that are characteristic for β-sheet directed assemblies. In fact, the negative band at λ = 200 nm, and weak positive band at λ = 218 nm are characteristic for a random-coil peptide

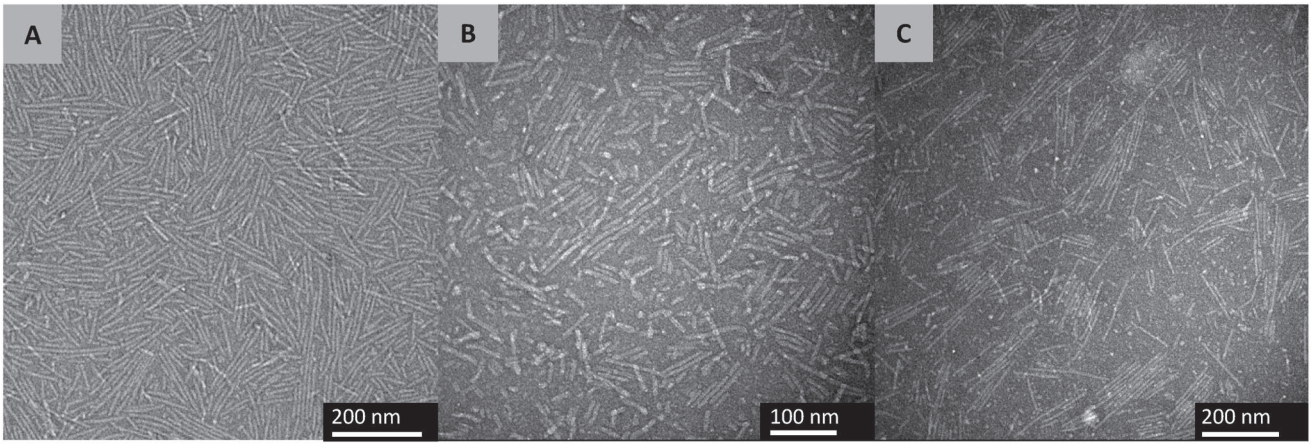

Figure 3. Negative stained TEM images with 50 μM solutions in 20 mM Tris buffer of A) I (pH 10.75), B) II (pH 1.64), and C) I + II (pH 7.00).

secondary structure, similar to the molecular dissolved state of **I** and **II**. We thereby conclude that the oxidation of thioethers to a racemic mixture of sulfoxides disrupts the formation of superstructures due to a combination of increased hydrophilicity in the oligopeptide chain, as well as an increase of the steric demand. Furthermore, we performed TEM experiments to confirm that supramolecular polymer formation of the oxidized monomers **I[O]**, **II[O]** and the mixed comonomers **I[O]** + **II[O]** is not possible (Figures S3, S21–S23, Supporting Information). In all cases, TEM micrographs show only small spherical structures in the 9–14 nm size range, most likely monomer or small oligomers, thus confirming conclusions from CD spectroscopy.

Importantly, we further performed time-dependent kinetic CD measurements for the oxidation process with preequilibrated homo- and copolymer solutions, at a constant overall monomer concentration (60 μM), constant temperature (40 °C) and variable H_2O_2 concentrations. First, we investigated the oxidation induced disassembly of supramolecular polymers of acid monomer **II**, in analogy to previously reported monomer **IV**. Most conveniently, the oxidation was performed using varying concentrations of H_2O_2. The oxidation induced disassembly was followed by time-dependent CD spectroscopy and the polymer specific CD band at $\lambda = 265$ nm was used to plot the kinetic data (**Figure 4**). Note, that we previously investigated monomer **IV** in great detail.[17] Stable supramolecular polymers in acidic pH were obtained at low concentration and supramolecular hydrogels at >0.5 wt%. The oxidation process was followed and confirmed by CD and NMR spectroscopy, HPLC chromatography, and the disassembly confirmed using TEM and rheology.[17] In case of acidic monomer **II**, the supramolecular homopolymers were obtained at pH values of 2.8–2.9 and the disassembly induced upon oxidation with H_2O_2. The superimposed kinetic data obtained from CD spectra for building block **II**, shows that by increasing the H_2O_2 concentration from 30 to 70 mM, the oxidative disassembly rate increases slightly as observed by a decrease in the half-life $t_{1/2}$ from 4 to 2.5 h (Figure 4A; Figures S9–S11, Supporting Information). Note, that $t_{1/2}$ was determined as the time at which the intensity of the CD band at 265 nm which is characteristic for the supramolecular polymer decreased to half of its original value. Interestingly, similar experiments for the basic lysine containing monomer **I** at pH = 10.1–10.6 showed a similar trend and decrease of $t_{1/2}$ from 10 h to 6 h. However, the oxidative disassembly rate is slower and at low H_2O_2 concentration of 30 mM, the process seems to be incomplete (Figure 4B; Figures S7 and S8, Supporting Information). Even at $t > 10$ h, the CD spectra do not match the ones expected for a molecular dissolved state. We refer to mechanistic investigations by Trout and coworkers that

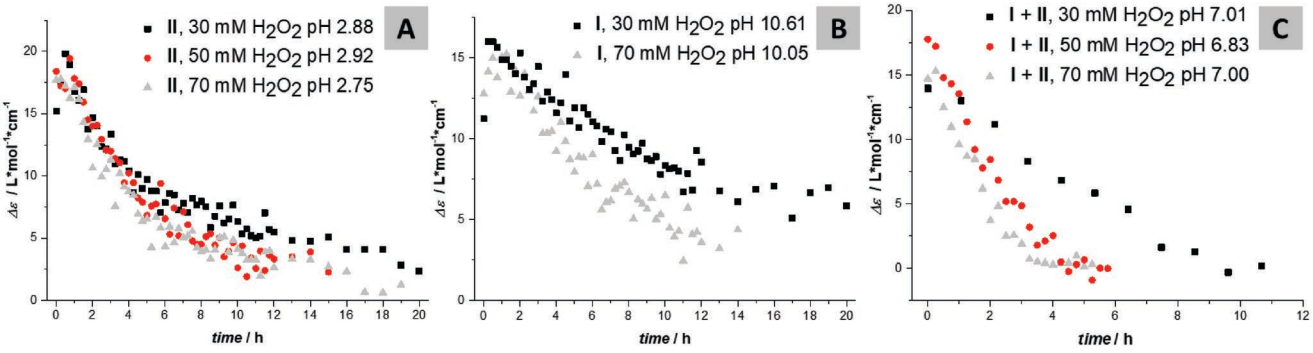

Figure 4. CD-spectroscopic investigation of the oxidative disassembly using building blocks II A), I B), I + II C) at an overall monomer concentration of 60 μM solutions in 10 mM phosphate buffer, in the presence of various amounts of H_2O_2 at 40 °C. The intensity of the supramolecular polymer CD band at $\lambda = 265$ nm was monitored against time (Figures S7–S14, Supporting Information).

report a pH independent rate constant for the oxidation of free methionine by H_2O_2 in a pH range between pH 2–8.[52,53] However, upon deprotonation of H_2O_2 (pK_a = 11.0), the conjugate base HO_2^- is a much weaker electrophile for the nucleophilic thioether reaction partner, and the oxidation rate of dimethylsulfide in water was reported to decrease by about an order of magnitude.[54] This might explain our observed decrease in oxidative disassembly for homopolymers of **I** at pH > 10.

We were pleased to observe that the supramolecular ampholytic copolymer of **I** + **II** shows the fastest response in the oxidative disassembly. Even at the lowest concentration of 30 mM H_2O_2, full disassembly was observed after 10 h (Figure 4C; Figures S12–S14, Supporting Information). The H_2O_2-dependent $t_{1/2}$, decreased from 3.2 h at the lowest to 1.2 h at the highest concentration, and the experiments were performed at neutral buffered pH values between 6.8 and 7.0. Using the comonomer pairs of **III** and **IV** we were able to confirm these results (Figures S6 and S15, Supporting Information). In case of the copolymers of **III** + **IV** and a H_2O_2 concentration of 30 mM, full disassembly was observed after 9.5 h and the $t_{1/2}$ value was 3.5 h. We hypothesize that the faster oxidation at neutral pH compared to the oxidation of homopolymers of **II** or **IV** at pH 3, is due to the fact that the charged cationic and anionic peptide side chains of copolymers of **I** + **II** and **III** + **IV**, increase the hydrophilicity of the β-sheet domains and thereby the accessibility for oxidizing agents like H_2O_2. These findings are supported by observations by Tirelli and coworkers on polysulfide-based block copolymer assemblies.[28] The rate of oxidative disassembly using H_2O_2 increased with the polarity of the thioether-based hydrophobic domains. We thereby conclude that co-assembly into multicomponent supramolecular polymers using a balance of charge regulation and hydrophobic shielding provides access to oxidation-responsive non-covalent superstructures with properties that are tuneable over a wider time scale compared to traditional amphiphilic self-assembled molecular or polymeric materials.

In summary, we have presented the synthesis of multi-stimuli-responsive supramolecular building blocks, using β-sheet subunits that are driven by a combination of charge screening and hydrogen bonding. Homo- and copolymerization processes into 1D nanorods in water are observed, using glutamic acid or lysine residues in either of the peptide comonomers **I–IV**. The incorporation of methionine as hydrophobic amino acid supports β-sheet formation, but oxidation of the thioether side-chain to a sulfoxide functional group destabilizes the β-sheet ordered domains. We have furthermore introduced a new water solubilizing Newkome type dendron, which reduces the required synthetic steps significantly from eight to five, and provides high colloidal stability to the supramolecular polymer nanorods. The oxidation induced disassembly of all monomer pairs was investigated in detail. Using H_2O_2 as ROS, we have probed the time scale and kinetics of the oxidation responsive supramolecular materials. ROS are known to play an important role in signaling cascades and inflammation processes. We have therefore been interested in developing strategies for the design of tuneable and responsive biomaterials for applications in redox microenvironments. In this study, we find that the oxidative disassembly of charged ampholytic copolymers is up to two times faster compared to the charge neutral homopolymers. Our findings are therefore important for the growing field of amphiphilic polythioether containing (macro) molecular building blocks, particularly in view of tuning their oxidation induced disassembly which tends to be notoriously slow, require high concentrations of ROS and acidic reaction media.

Experimental Section

For full experimental details, synthetic procedures, molecular characterization, and instrumentation details, see Supporting Information.

CD measurements were carried out on a JASCO J-815 spectrometer equipped with Spectra Manager 2.12.00. Unless not otherwise stated, all sample measurements were buffer-corrected in advance and measured at 20 °C controlled by a Jasco PTC-423S/15 peltier-element. Moreover, each measurement was repeated at least three times. In time-dependent measurements, the samples were measured every 15 min or 64 min at 40 °C in a period of 5–20 h. The concentrations were adjusted to keep the photomultiplier's high voltage (HV) below 600 V in the wavelength area of interest (λ > 215 nm). The pH values were adjusted by addition of diluted aqueous HCl and NaOH and afterward measured with a MI-410 (Microelectrodes, Inc.) pH-electrode. The data was analyzed using OriginPro 9.1.

TEM images were obtained on a FEI Tecnai T12 transmission electron microscope equipped with a BioTWIN lens and a LaB_6 cathode operated at 120 kV. Samples were prepared on freshly glow-discharged copper grids (CF300-Cu, 300 mesh, *Electron Microscopy Sciences*) coated with a 3–4 nm carbon layer. Thereto, 5 µL samples were allowed to deposit on the grid for 1 min and excess solvent was afterward carefully removed with Whatman No. 4 filter papers. Subsequently, the samples were negatively stained by incubation with a 5 µL drop of 2 vol% solution of uranyl acetate for 15 s prior to the measurement. Digital electron micrographs were recorded with a *TVIPS* 4k × 4k CMOS camera and a MEGASSYS 1k × 1k CCD camera.

Supporting Information

Supporting Information is available from the Wiley Online Library or from the author.

Acknowledgements

C.M.B. is the recipient of a position through the DFG Excellence Initiative by the Graduate School Materials Science in Mainz (GSC 266). L.Z. is the recipient of a Werner Schwarze scholarship from the Evonik Foundation.

Conflict of Interest

The authors declare no conflict of interest.

Keywords

kinetic control, multicomponent supramolecular polymers, reactive oxygen species responsive materials, redox regulation, supramolecular chemistry

Received: September 4, 2019
Revised: September 25, 2019
Published online: November 4, 2019

[1] J. M. Lehn, *Science* **2002**, *295*, 2400.
[2] G. M. Whitesides, B. Grzybowski, *Science* **2002**, *295*, 2418.
[3] E. Mattia, S. Otto, *Nat. Nanotechnol.* **2015**, *10*, 111.
[4] B. A. Grzybowski, W. T. S. Huck, *Nat. Nanotechnol.* **2016**, *11*, 585.
[5] S. A. P. van Rossum, M. Tena-Solsona, J. H. van Esch, R. Eelkema, J. Boekhoven, *Chem. Soc. Rev.* **2017**, *46*, 5519.
[6] R. Merindol, A. Walther, *Chem. Soc. Rev.* **2017**, *46*, 5588.
[7] A. Sorrenti, J. Leira-Iglesias, A. J. Markvoort, T. F. A. de Greef, T. M. Hermans, *Chem. Soc. Rev.* **2017**, *46*, 5476.
[8] J. Leira-Iglesias, A. Tassoni, T. Adachi, M. Stich, T. M. Hermans, *Nat. Nanotechnol.* **2018**, *13*, 1021.
[9] G. Vantomme, E. W. Meijer, *Science* **2019**, *363*, 1396.
[10] J. Baram, E. Shirman, N. Ben-Shitrit, A. Ustinov, H. Weissman, I. Pinkas, S. G. Wolf, B. Rybtchinski, *J. Am. Chem. Soc.* **2008**, *130*, 14966.
[11] J. W. Sadownik, R. V Ulijn, *Chem. Commun.* **2010**, *46*, 3481.
[12] R. V. Ulijn, P. F. Caponi, *Nat. Chem.* **2010**, *2*, 521.
[13] B. Rybtchinski, *ACS Nano* **2011**, *5*, 6791.
[14] H. Frisch, J. P. Unsleber, D. Lüdeker, M. Peterlechner, G. Brunklaus, M. Waller, P. Besenius, *Angew. Chem., Int. Ed.* **2013**, *52*, 10097.
[15] D. W. R. Balkenende, S. Coulibaly, S. Balog, Y. C. Simon, G. L. Fiore, C. Weder, *J. Am. Chem. Soc.* **2014**, *136*, 10493.
[16] S. Dhiman, A. Jain, M. Kumar, S. J. George, *J. Am. Chem. Soc.* **2017**, *139*, 16568.
[17] D. Spitzer, L. L. Rodrigues, D. Strassburger, M. Mezger, P. Besenius, *Angew. Chem., Int. Ed.* **2017**, *56*, 15461.
[18] M. Von Gröning, I. De Feijter, M. C. A. Stuart, I. K. Voets, P. Besenius, *J. Mater. Chem. B* **2013**, *1*, 2008.
[19] H. Frisch, J. P. Unsleber, D. Lüdeker, M. Peterlechner, G. Brunklaus, M. Waller, P. Besenius, *Angew. Chem., Int. Ed.* **2013**, *52*, 10097.
[20] P. Ahlers, H. Frisch, P. Besenius, *Polym. Chem.* **2015**, *6*, 7245.
[21] P. Ahlers, K. Fischer, D. Spitzer, P. Besenius, *Macromolecules* **2017**, *50*, 7712.
[22] R. Otter, C. M. Berac, S. Seiffert, P. Besenius, *Eur. Polym. J.* **2019**, *110*, 90.
[23] H. G. Batz, V. Hofmann, H. Ringsdorf, *Makromol. Chem.* **1973**, *169*, 323.
[24] G. P. Dado, S. H. Gellman, *J. Am. Chem. Soc.* **1993**, *115*, 12609.
[25] L. Hu, L. P. de la Rama, M. Y. Efremov, Y. Anahory, F. Schiettekatte, L. H. Allen, *J. Am. Chem. Soc.* **2011**, *133*, 4367.
[26] P. Carampin, E. Lallana, J. Laliturai, S. C. Carroccio, C. Puglisi, N. Tirelli, *Macromol. Chem. Phys.* **2012**, *213*, 2052.
[27] M. K. Gupta, T. A. Meyer, C. E. Nelson, C. L. Duvall, *J. Controlled Release* **2012**, *162*, 591.
[28] R. d'Arcy, A. Siani, E. Lallana, N. Tirelli, *Macromolecules* **2015**, *48*, 8108.
[29] M. Tang, P. Hu, Q. Zheng, N. Tirelli, X. Yang, Z. Wang, Y. Wang, Q. Tang, Y. He, *J. Nanobiotechnol.* **2017**, *15*, 39.
[30] F. El-Mohtadi, R. D'Arcy, N. Tirelli, *Macromol. Rapid Commun.* **2019**, *40*, 1800699.
[31] A. Napoli, M. Valentini, N. Tirelli, M. Müller, J. A. Hubbell, *Nat. Mater.* **2004**, *3*, 183.
[32] A. Napoli, M. J. Boerakker, N. Tirelli, R. J. M. Nolte, N. A. J. M. Sommerdijk, J. A. Hubbell, *Langmuir* **2004**, *20*, 3487.
[33] A. Rehor, N. E. Botterhuis, J. A. Hubbell, N. A. J. M. Sommerdijk, N. Tirelli, *J. Mater. Chem.* **2005**, *15*, 4006.
[34] A. Rehor, J. A. Hubbell, N. Tirelli, *Langmuir* **2005**, *21*, 411.
[35] C. E. Brubaker, D. Velluto, D. Demurtas, E. A. Phelps, J. A. Hubbell, *ACS Nano* **2015**, *9*, 6872.
[36] J. R. Kramer, T. J. Deming, *Biomacromolecules* **2012**, *13*, 1719.
[37] A. R. Rodriguez, J. R. Kramer, T. J. Deming, *Biomacromolecules* **2013**, *14*, 3610.
[38] A. R. Rodriguez, U.-J. Choe, D. T. Kamei, T. J. Deming, *Macromol. Biosci.* **2015**, *15*, 90.
[39] J. Herzberger, K. Fischer, D. Leibig, M. Bros, R. Thiermann, H. Frey, *J. Am. Chem. Soc.* **2016**, *138*, 9212.
[40] N. Brot, H. Weissbach, *Trends Biochem. Sci.* **1982**, *7*, 137.
[41] N. Brot, H. Weissbach, *Arch. Biochem. Biophys.* **1983**, *223*, 271.
[42] E. R. Stadtman, J. Moskovitz, R. L. Levine, *Antioxid. Redox Signaling* **2003**, *5*, 577.
[43] S. H. Lee, M. K. Gupta, J. B. Bang, H. Bae, H.-J. Sung, *Adv. Healthcare Mater.* **2013**, *2*, 908.
[44] A. Stano, E. A. Scott, K. Y. Dane, M. A. Swartz, J. A. Hubbell, *Biomaterials* **2013**, *34*, 4339.
[45] N. B. Karabin, S. Allen, H.-K. Kwon, S. Bobbala, E. Firlar, T. Shokuhfar, K. R. Shull, E. A. Scott, *Nat. Commun.* **2018**, *9*, 624.
[46] G. R. Newkome, C. Shreiner, *Chem. Rev.* **2010**, *110*, 6338.
[47] S. Engel, D. Spitzer, L. L. Rodrigues, E. C. Fritz, D. Strassburger, M. Schoenhoff, B. J. Ravoo, P. Besenius, *Faraday Discuss.* **2017**, *204*, 53.
[48] R. Appel, J. Fuchs, S. M. Tyrrell, P. A. Korevaar, M. C. A. Stuart, I. K. Voets, M. Schönhoff, P. Besenius, *Chem. - Eur. J.* **2015**, *21*, 19257.
[49] H. C. Kolb, M. G. Finn, K. B. Sharpless, *Angew. Chem., Int. Ed.* **2001**, *40*, 2004.
[50] C. W. Tornøe, C. Christensen, M. Meldal, *J. Org. Chem.* **2002**, *67*, 3057.
[51] H. Frisch, Y. Nie, S. Raunser, P. Besenius, *Chem. - Eur. J.* **2015**, *21*, 3304.
[52] J.-W. Chu, B. L. Trout, *J. Am. Chem. Soc.* **2004**, *126*, 900.
[53] J. Chu, J. Yin, B. R. Brooks, D. I. C. Wang, M. S. Ricci, D. N. Brems, B. L. Trout, *J. Pharm. Sci.* **2004**, *93*, 3096.
[54] P. Amels, H. Elias, K.-J. Wannowius, *J. Chem. Soc., Faraday Trans.* **1997**, *93*, 2537.